mathematics

MDPI

Article

Taxis-Driven Pattern Formation in Tri-Trophic Food Chain Model with Omnivory

Evgeniya Giricheva

Institute of Automation and Control Processes, Far Eastern Branch of the Russian Academy of Science, 5 Radio Street, Vladivostok 690014, Russia; evg.giricheva@yandex.ru

Abstract: The spatiotemporal dynamics of a three-component model of a food web are considered. The model describes the interactions between populations of resources, prey, and predators that consume both species. It assumes that the predator responds to the spatial change in the resource and prey densities by occupying areas where species density is higher (prey-taxis) and that the prey population avoids areas with a high predator density (predator-taxis). This work studies the conditions for the taxis-driven instability leading to the emergence of stationary patterns resulting from Turing instability and autowaves caused by wave instability. The existence of nonconstant positive steady states for the system is assessed through a rigorous bifurcation analysis. Meanwhile, the conditions for the existence of both types of instabilities are obtained by linear stability analysis. It is shown that the presence of cross-diffusion in the system supports the formation of spatially heterogeneous patterns. For low values of the resource-tactic and predator-tactic coefficients, Turing and wave instabilities coexist. The system undergoes only Turing instability for high levels of these parameters.

Keywords: food web model; prey- and predator-taxis; nonconstant positive steady states; Turing and wave instability; pattern formation

MSC: 37N30; 35B32; 92D25

Citation: Giricheva, E. Taxis-Driven Pattern Formation in Tri-Trophic Food Chain Model with Omnivory. *Mathematics* **2024**, *12*, 290. https://doi.org/10.3390/math12020290

Academic Editor: Giancarlo Consolo

Received: 13 December 2023
Revised: 8 January 2024
Accepted: 15 January 2024
Published: 16 January 2024

1. Introduction

An ecological community is a part of an ecosystem containing different species of organisms interacting in space and time. The need to consider the spatial organization of a community along with its trophic structure is recognized in mathematical ecology and has been the subject of analysis in the modeling of ecological systems over the past decades. The interplay between trophic and spatial heterogeneity might induce contrasting effects depending on the internal dynamics of the system [1,2].

Among the mathematical tools for studying spatiotemporal processes in ecosystems are partial differential equations (PDEs). PDE models allow the description of numerous fundamental population processes such as dispersal, ecological invasions, dispersal-mediated coexistence, and emergence of spatial patterns [3]. Skellam's analogy [4] between the movement of molecules and the random movements of individual members of biological species gave impetus to the use of reaction–diffusion models in theoretical ecology.

Diffusive predator–prey models assume that species move randomly in their habitats. However, in real predator–prey communities, directed movements of predator and prey populations often occurs, which is usually shown by the predator pursuing the prey and the prey escaping from the predator. The spatial behavior of the predator moving toward the gradient direction of the prey distribution is classified as prey-taxis. Predator-taxis means that the prey moves opposite to the gradient of the predator distribution.

Starting with the classical model [5], directed movement of predators has attracted much attention in recent years and has inspired numerous works on population dynamics

models of one-predator and one-prey systems with prey-taxis [6–9]. These studies analyzed the prey-taxis effects on pattern formation when a spatially homogeneous equilibrium loses its stability. In [10], necessary conditions for pattern formation with diverse prey birth rates, predator mortality rates, and functional responses were investigated. The authors found that with an increase in the taxis coefficient, spatial structures disappeared, and the system stabilized. However, the taxis role as a stabilizing factor is unobvious. It is generally accepted that the ability for self-organization of a system is determined by nonlinear trophic functions. However, [11] provided a method for modeling spatial patterns emerging in trophic systems due to the directed movements of the consumer species.

The influence of taxis on system dynamics has also been studied for three-species systems. In [12], a model of a two-predator–one-prey ecosystem with cross-diffusion and a prey defense mechanism was considered. The authors obtained conditions for the emergence of stationary inhomogeneous structures with an increasing taxis coefficient. The work [13] also modeled a system in which two predators consume one prey, and the prey-taxis of both predators can be either positive or negative. Negative taxis was interpreted as a predator's avoidance of areas where the prey population accumulates because prey can defend themselves as a group (see [14,15]). The authors established that the formation of stationary and periodic structures is possible when the taxis of one predator is positive and that of the other is negative.

The interactions among more than two species are modeled by food chain models. Various types of food chain models consisting of three species are available: one of which is a food chain with omnivory. A special kind of omnivory known as intraguild predation [16] is characterized by predators that feed on one or more of the resources of their own prey. This approach can be applied to model a tritrophic food chain, such as a planktivorous fish that feeds on planktonic food, including phytoplankton and zooplankton, or herbivorous and carnivorous zooplankton [17,18]. A similar model can describe the interaction between phytoplankton, microzooplankton, and mesozooplankton.

This study continues the analysis of the nonspatial model [19] proposed by the author and takes into account the spatial movements of species. The presented model considers relationships between the resource, prey, and a predator that feeds on both species. This model differs from previous ones in that the predator's functional response depends on the density of one species. The use of a one-prey functional responses allows us to model the various feeding behaviors of predators that can shift from one feeding mode to another. The previous study revealed that the proposed model with self-limitation of the prey or predators and saturated consumption of them can reproduce coexistence between the three species in a resource-rich environment. Additionally, the model considers movement of the predator toward the gradient direction of both species' distributions and the anti-predator behavior of prey moving away from the direction with a high predator density. Recently, Wu et al. [20] investigated the global existence of and the boundedness in a reaction–diffusion model with predator-taxis and showed that the presence of predator-taxis can induce the disappearance of spatial patterns. Fuest [21] investigated global solutions and convergence near homogeneous steady states in a spatial predator–prey model with predator- and prey-taxis. The spatiotemporal patterns in a predator–prey model including predator- and prey-taxis were studied by Wang et al. [22].

A number of works [13,23,24] studying the effect of taxis on the model dynamics state the stabilizing role of this factor in the case of positive values and the possibility of pattern formation in the case of negative ones. The purpose of this study is to determine the effects of positive prey-taxis and negative predator-taxis on the spatiotemporal dynamics of the system and pattern formation. The reason for the Turing pattern occurrence is the existence of nonconstant positive steady states of a model as a result of diffusion. Stationary structures can also be formed under the influence of taxis pressure. The system's ability to self-organize into spatial patterns forms a mechanism of species coexistence. Through biodiversity conservation, therefore, the influence of taxis pressure on the existence of nonconstant positive solutions is of interest as the coexistence mechanism.

The remainder of this paper is organized as follows: Section 2 introduces a model of a food chain and its dimensionless form. In Section 3, the linear bifurcation analysis is carried out and the existence of a nonconstant positive equilibrium is investigated. In Section 4, the conditions for Turing and wave instabilities are obtained. Pattern formation is numerically illustrated in Section 5.

2. Model Formulation and Preliminary Analysis

The model consists of three coupled partial differential equations describing the changes to the densities of the resource $R(x,t)$, prey $N(x,t)$, and predator $P(x,t)$ at time t and position x:

$$\begin{array}{ll} \frac{\partial R}{\partial t} = D_1\Delta R + f_1(R,N,P), & x \in \Omega, \\ \frac{\partial N}{\partial t} = D_2\Delta N + \nabla(N\chi_P\nabla P) + f_2(R,N,P), & x \in \Omega, \\ \frac{\partial P}{\partial t} = D_3\Delta P - \nabla(P\nabla(\chi_R R + \chi_N N)) + f_3(R,N,P), & x \in \Omega, \\ \nabla R = \nabla N = \nabla P = 0, & x \in \partial\Omega. \end{array} \tag{1}$$

Here, $\Omega = [0, L]$, and a homogeneous Neumann boundary condition is imposed to describe an enclosed domain; D_i are the diffusion coefficients. The term $\nabla(N\chi_P\nabla P)$ shows the tendency of prey to move away from the high gradient of predator density with taxis rate $\chi_P \geq 0$, and the term $\nabla(P\nabla(\chi_R R + \chi_N N))$ shows the tendency of predators to move towards the direction of resource and prey gradients with rates χ_R and χ_N, respectively. The nonlinear functions $f_i(R,N,P)$ represent the interactions between the predators, prey, and resources as follows:

$$\begin{array}{l} f_1(R,N,P) = rR\left(1 - \frac{R}{K}\right) - \frac{\mu_1 RN}{K_1+R} - \frac{\mu_2 RP}{K_2+R}, \\ f_2(R,N,P) = \frac{\alpha_1\mu_1 RN}{K_1+R} - \frac{\mu_3 NP}{K_3+N} - m_1 N - \delta_1 N^2, \\ f_3(R,N,P) = \frac{\alpha_2\mu_2 RP}{K_2+R} + \frac{\alpha_3\mu_3 NP}{K_3+N} - m_2 P - \delta_2 P^2. \end{array} \tag{2}$$

Here, r is the maximum growth rate of the resource population, K is the resource carrying capacity, μ_i and K_i are the predation rates and half-saturation constants of prey and predator; α_i are the assimilation coefficients, and m_i and δ_i are the rates of natural mortality and intraspecies predation of prey and predator, respectively. All the parameters are assumed to be positive.

Introducing the dimensionless variables and parameters

$$\begin{array}{l} \bar{t} = rt, \quad \bar{x} = xL, \quad u = \frac{R}{K}, \quad v = \frac{\mu_1}{rK}N, \quad w = \frac{\mu_2}{rK}P, \quad d_i = \frac{D_i}{rL^2}, \\ \chi_1 = \frac{K}{\mu_2 L^2}\chi_P, \quad \chi_2 = \frac{K}{r\mu_2 L^2}\chi_R, \quad \chi_3 = \frac{K}{\mu_1 L^2}\chi_N, \\ \gamma_1 = \frac{K_1}{K}, \quad \gamma_2 = \frac{K_2}{K}, \quad \gamma_3 = \frac{K_3\mu_1}{rK}, \quad \bar{\mu}_1 = \frac{\alpha_1\mu_1}{r}, \quad \bar{\mu}_2 = \frac{\alpha_2\mu_2}{r}, \quad \bar{\mu}_3 = \frac{\mu_1\mu_3}{\mu_2}, \quad \bar{\mu}_4 = \frac{\alpha_3\mu_3}{r}, \\ \bar{m}_1 = \frac{m_1}{r}, \quad \bar{m}_2 = \frac{m_2}{r}, \quad \bar{\delta}_1 = \frac{\delta_1 K}{\mu_1}, \quad \bar{\delta}_2 = \frac{\delta_2 K}{\mu_2} \end{array}$$

and dropping the over-bars, we obtain the nondimensional model as

$$\begin{array}{ll} \frac{\partial u}{\partial t} = d_1\frac{\partial^2 u}{\partial x^2} + f(u,v,w), & x \in \Omega, t > 0, \\ \frac{\partial v}{\partial t} = d_2\frac{\partial^2 v}{\partial x^2} + \frac{\partial}{\partial x}\left(\chi_1 v\frac{\partial w}{\partial x}\right) + g(u,v,w), & x \in \Omega, t > 0, \\ \frac{\partial w}{\partial t} = d_3\frac{\partial^2 w}{\partial x^2} - \frac{\partial}{\partial x}\left(w(\chi_2\frac{\partial u}{\partial x} + \chi_3\frac{\partial v}{\partial x})\right) + h(u,v,w), & x \in \Omega, t > 0, \\ \frac{\partial u}{\partial x} = \frac{\partial v}{\partial x} = \frac{\partial w}{\partial x} = 0, & x \in \partial\Omega, t > 0. \end{array} \tag{3}$$

Here, $\Omega = [0, 1]$ and

$$\begin{array}{l} f(u,v,w) = u(1-u) - \frac{uv}{\gamma_1+u} - \frac{uw}{\gamma_2+u}, \\ g(u,v,w) = \frac{\mu_1 uv}{\gamma_1+u} - \frac{\mu_3 vw}{\gamma_3+v} - m_1 v - \delta_1 v^2, \\ h(u,v,w) = \frac{\mu_2 uw}{\gamma_2+u} + \frac{\mu_4 vw}{\gamma_3+v} - m_2 w - \delta_2 w^2. \end{array} \tag{4}$$

The spatially homogeneous non-negative steady states of System (3) are given by: $E_0 = (0,0,0)$, $E_1 = (1,0,0)$, $E_2 = (u_2, v_2, 0)$, and $E_3 = (u_3, 0, w_3)$, where

$$v_2 = (1-u_2)(\gamma_1 + u_2), \quad w_3 = (1-u_3)(\gamma_2 + u_3), \tag{5}$$

and u_2, u_3 are positive roots of the following equations:

$$\begin{aligned} &\mu_1 u_2 - (\gamma_1 + u_2)(m_1 + \delta_1(1-u_2)(\gamma_1 + u_2)) = 0, \\ &\mu_2 u_3 - (\gamma_2 + u_3)(m_2 + \delta_2(1-u_3)(\gamma_2 + u_3)) = 0. \end{aligned} \tag{6}$$

The positive steady state is given by $E^* = (u^*, v^*, w^*)$, where

$$w^* = \frac{\gamma_3 + v^*}{\mu_3(\gamma_1 + u^*)}[u^*(\mu_1 - m_1) - \gamma_1 m_1 - \delta_1(\gamma_1 + u^*)v^*], \tag{7}$$

v^* is a positive root of the equation:

$$\begin{aligned} &\delta_1\delta_2(\gamma_1 + u^*)(v^*)^2 + [(\gamma_1 + u^*)(\mu_2\mu_3 u^* + \mu_3\mu_4) - \mu_1\delta_2(\gamma_2 + u^*)u^* + \\ &(\gamma_1 + u^*)(\gamma_2 + u^*)(\delta_1\delta_2(1+\gamma_3) - \mu_3 m_2)]v^* - \delta_2\gamma_3(\gamma_2 + u^*)(u^*(\mu_1 - m_1) - \gamma_1 m_1) = 0, \end{aligned} \tag{8}$$

and u^* is a positive root of the following equation:

$$\mu_3(\gamma_1 + u^*)(1-u^*) - \mu_3 v^* - (\gamma_3 + v^*)[u^*(\mu_1 - m_1) - \gamma_1 m_1 - \delta_1(\gamma_1 + u^*)v^*] = 0. \tag{9}$$

Proposition 1. *We have the following results:*

1. *There exist equilibria E_0 and E_1 for any parameters.*
2. *There exists equilibrium E_2 if $\mu_1 > m_1(1+\gamma_1)$.*
3. *There exists equilibrium E_3 if $\mu_2 > m_2(1+\gamma_2)$.*
4. *There exists equilibrium E^* if $\mu_1 > m_1$ and Equation (9) has a positive root u^* such that the following conditions are satisfied:*

$$u^* > \frac{\gamma_1 m_1}{\mu_1 - m_1}, \quad v^* < \frac{u^*(\mu_1 - m_1) - \gamma_1 m_1}{\delta_1(\gamma_1 + u^*)}. \tag{10}$$

Proof. Let us prove the existence of E_2. The first equation in (6) can be rewritten as

$$H(u_2) = \delta_1 u_2^3 + \delta_1(2\gamma_1 - 1)u_2^2 + (\mu_1 - m_1 + \delta_1\gamma_1(\gamma_1 - 2))u_2 - \gamma_1(m_1 + \delta_1\gamma_1)) = 0. \tag{11}$$

Note that $H(u_2 = 0) < 0$ and $H(u_2 = 1) > 0$ when $\mu_1 > m_1(1+\gamma_1)$. Then, there exists $\hat{u}_2 \in (0,1)$ such that $H(\hat{u}_2) = 0$. From (5), we have $v_2(\hat{u}_2) > 0$. The proof of the existence of E_3 is similar to the previous case. The existence of E^* follows directly from (7), (8), and (10). □

3. Classical Bifurcation Analysis

The main purpose of this section is to investigate the bifurcation structure of positive solutions to System (3) by regarding χ_3 as a bifurcation parameter and fixing all other parameters.

3.1. Linear Analysis

Let $E^* = (u^*, v^*, w^*)$ be a positive homogeneous equilibrium of System (3). Linearizing System (3) about E^* gives

$$\begin{aligned} &\dot{\overline{W}} = Q\Delta\overline{W} + J\overline{W}, && x \in \Omega, t > 0, \\ &\overline{W}' = 0, && x \in \partial\Omega, t > 0. \end{aligned} \tag{12}$$

Here, $\overline{W} = (\overline{u}, \overline{v}, \overline{w})^T$ are small spatiotemporal perturbations away from $E^* = (u^*, v^*, w^*)$, and

$$Q = \begin{pmatrix} d_1 & 0 & 0 \\ 0 & d_2 & \chi_1 v^* \\ -\chi_2 w^* & -\chi_3 w^* & d_3 \end{pmatrix}.$$

The Jacobian matrix evaluated at E^* is:

$$J = \begin{pmatrix} f_u^* & f_v^* & f_w^* \\ g_u^* & g_v^* & g_w^* \\ h_u^* & h_v^* & h_w^* \end{pmatrix}, \tag{13}$$

where $f_u^* = f_u'(u^*, v^*, w^*)$ and $f_u^* = 1 - 2u^* - \frac{\gamma_1 u}{(\gamma_1+u)^2} - \frac{\gamma_2 w}{(\gamma_2+u)^2}$, $f_v^* = -\frac{u^*}{\gamma_1+u^*}$, $f_w^* = -\frac{u^*}{\gamma_2+u^*}$, $g_u^* = \frac{\mu_1\gamma_1 v^*}{(\gamma_1+u^*)^2}$, $g_v^* = \frac{\mu_3 v^* w^*}{(\gamma_3+v^*)^2} - \delta_1 v^*$, $g_w^* = -\frac{\mu_3 v^*}{\gamma_3+v^*}$, $h_u^* = \frac{\mu_2\gamma_2 w^*}{(\gamma_2+u^*)^2}$, $h_v^* = \frac{\mu_4\gamma_3 w^*}{(\gamma_3+v^*)^2}$, $h_w^* = -\delta_2 w^*$.

Since $\Omega = [0, 1]$, the solutions for System (12) can be expanded into a Fourier series [25]:

$$\overline{W} = \sum_{k=0}^{\infty} W_k e^{\lambda_k t} \cos kx, \quad k = n\pi, n \in \mathbb{N}^+, \tag{14}$$

where W_k are the Fourier coefficients, λ_k denotes the growth rate of the solution, and k is the wavenumber corresponding to mode number n. Substituting (14) into (12) leads to the following system:

$$M_k \cdot W_k^T = 0, \qquad M_k = \lambda_k E + k^2 Q - J.$$

The characteristic equation for the above system can be written as:

$$\phi(\lambda_k) = \lambda_k^3 + r_2(k^2)\lambda_k^2 + r_1(k^2)\lambda_k + r_0(k^2) = 0, \tag{15}$$

where

$$\begin{aligned} r_2(k^2) &= s_{21}k^2 + p_2, \\ r_1(k^2) &= s_{12}(k^2)^2 + s_{11}k^2 + p_1, \\ r_0(k^2) &= s_{03}(k^2)^3 + s_{02}(k^2)^2 + s_{01}k^2 + p_0, \end{aligned}$$

with $p_2 = -(f_u^* + g_v^* + h_w^*)$, $p_1 = f_u^* g_v^* + f_u^* h_w^* + g_v^* h_w^* - f_v^* g_u^* - f_w^* h_u^* - g_w^* h_v^*$, $p_0 = f_u^* g_w^* h_v^* + f_v^* g_u^* h_w^* + f_w^* g_v^* h_u^* - f_u^* g_v^* h_w^* - f_v^* g_w^* h_u^* - f_w^* g_u^* h_v^*$, and

$$\begin{aligned} s_{21} &= d_1 + d_2 + d_3, \quad s_{12} = d_1 d_2 + d_1 d_3 + d_2 d_3 + \chi_1\chi_3 v^* w^*, \quad s_{03} = d_1 d_2 d_3 + d_1\chi_1\chi_3 v^* w^*, \\ s_{11} &= -(d_1(g_v^* + h_w^*) + d_2(f_u^* + h_w^*) + d_3(f_u^* + g_v^*) + w^*(\chi_2 f_w^* + \chi_3 g_w^*) - \chi_1 v^* h_v^*), \\ s_{02} &= -(d_2 d_3 f_u^* + d_1 d_3 g_v^* + d_1 d_2 h_w^* + w^*(\chi_2(d_2 f_w^* - \chi_1 v^* f_v^*) + \chi_3(d_1 g_w^* + \chi_1 v^* f_u^*)) - \chi_1 v^* d_1 h_v^*), \\ s_{01} &= d_1(g_v^* h_w^* - g_w^* h_v^*) + d_2(f_u^* h_w^* - f_w^* h_u^*) + d_3(f_u^* g_v^* - f_v^* g_u^*) + \\ &\quad \chi_1 v^*(f_v^* g_u^* - f_u^* h_v^*) + w^*(\chi_2(f_w^* g_v^* - f_v^* g_w^*) + \chi_3(f_u^* g_w^* - f_w^* g_u^*)). \end{aligned}$$

According to the Routh–Hurwitz criteria, the equilibrium point E^* is stable with respect to spatially homogeneous and nonhomogeneous perturbations if the following conditions hold:

$$r_2(k^2) > 0, \quad r_0(k^2) > 0, \quad r_2(k^2)r_1(k^2) - r_0(k^2) > 0, \qquad k^2 \geq 0. \tag{16}$$

The local stability of the positive equilibrium E^* for the homogeneous model is a necessary condition for Turing and wave instability. Let $p_2 > 0, p_0 > 0, p_2 p_1 - p_0 > 0$; then (16) are satisfied for $k = 0$, and E^* is the stable homogeneous stationary state. Moreover, $r_2(k^2) > 0$. The equilibrium loses its stability if one of the two remaining conditions in (16) is violated. If $r_0(k^2) < 0$ for some $k^2 > 0$, then Equation (15) has one positive real root: this implies that Turing instability occurs, and there exist nonconstant positive steady states for System (3). If $r_2(k^2)r_1(k^2) - r_0(k^2) < 0$ for some $k^2 > 0$, then Equation (15) has a pair of complex roots with a positive real part: this means that wave instability occurs.

3.2. Existence of Nonconstant Positive Steady States

In this subsection, the existence of a nonconstant interior equilibrium is considered. In the following, the bifurcation theory of Crandall–Rabinovitz [26] and its application to the bifurcation analysis of elliptic systems developed in [27] are applied to prove the existence of a Turing bifurcation with χ_3 as the bifurcation parameter. I study a positive nonconstant solution for the following system:

$$\begin{array}{ll} d_1u'' + f(u,v,w) = 0, & x \in \Omega, t > 0, \\ d_2v'' + (\chi_1 v w')' + g(u,v,w), & x \in \Omega, t > 0, \\ d_3w'' - (w(\chi_2 u' + \chi_3 v'))' + h(u,v,w), & x \in \Omega, t > 0, \\ u' = v' = w' = 0, & x \in \partial\Omega, t > 0. \end{array} \tag{17}$$

Here, prime denotes differentiation with respect to x. System (17) can be rewritten in the following form:

$$\mathcal{F}(u,v,w,\chi_3) = 0, \quad (u,v,w,\chi_3) \in \mathcal{X} \times \mathcal{X} \times \mathcal{X} \times \mathbb{R}, \tag{18}$$

where

$$\mathcal{F}(u,v,w,\chi) = \begin{pmatrix} d_1u'' + f(u,v,w) \\ d_2v'' + (\chi_1 v w')' + g(u,v,w) \\ d_3w'' - (w(\chi_2 u' + \chi_3 v'))' + h(u,v,w) \end{pmatrix}, \tag{19}$$

and

$$\mathcal{X} = \{z \in H^2(0,1) | z'(0) = z'(1) = 0\}.$$

Then, for fix $\chi_3 \in \mathbb{R}$, any solution (u,v,w) of (18) is a classical solution for (17).

Note that $\mathcal{F} : \mathcal{X} \times \mathcal{X} \times \mathcal{X} \times \mathbb{R} \to \mathcal{Y} \times \mathcal{Y}$, $\mathcal{Y} = L^2(0,1)$ is a continuously differentiable mapping, and $\mathcal{F}(u^*, v^*, w^*, \chi_3) = 0$ for any $\chi_3 \in \mathbb{R}$. The Fréchet derivative of $\mathcal{F}$ for any $(\tilde{u}, \tilde{v}, \tilde{w})$ is given by

$$D_{(u,v,w)}\mathcal{F}(\tilde{u},\tilde{v},\tilde{w},\chi_3)(u,v,w) = \begin{pmatrix} d_1u'' + \tilde{f}_u u + \tilde{f}_v v + \tilde{f}_w w \\ d_2v'' + \chi_1(\tilde{v}w' + \tilde{w}'v)' + \tilde{g}_u u + \tilde{g}_v v + \tilde{g}_w w \\ d_3w'' - \chi_2(\tilde{w}u' + \tilde{u}'w)' - \chi_3(\tilde{w}v' + \tilde{v}'w)' + \tilde{h}_u u + \tilde{h}_v v + \tilde{h}_w w \end{pmatrix}, \tag{20}$$

where $\tilde{f} = f(\tilde{u}, \tilde{v}, \tilde{w})$.

Theorem 1. *Suppose that all parameters in (17) are positive and there exists a positive constant equilibrium $E^* = (u^*, v^*, w^*)$. Assume that*

$$\begin{array}{l} k^2j^2((k^2+j^2)(A_1B_3 - A_3B_1) + k^2j^2(A_1B_2 - A_2B_1) + A_2B_3 - A_3B_2) \neq \\ p_0((k^4 + k^2j^2 + j^4)B_1 + (k^2+j^2)B_2 + B_3), \\ k, j > 0, \quad k \neq j. \end{array} \tag{21}$$

Here, A_i, B_j can be found in the proof of the theorem.

If there exists some $k > 0$ such that χ_k defined in (26) is positive, then there exists a constant $\epsilon > 0$ such that System (17) with $\chi_3 = \chi_k$ admits nonconstant positive solutions $(u_k(s,x), v_k(s,x), w_k(s,x), \chi_k(s))$ for $s \in (-\epsilon, \epsilon)$ that bifurcate from (u^*, v^*, w^*, χ_k), where both $\chi_k(s) \in \mathbb{R}$ and $(u_k(s,x), v_k(s,x), w_k(s,x)) \in \mathcal{X} \times \mathcal{X} \times \mathcal{X}$ are smooth functions of s. Furthermore, all nonconstant solutions of (17) must stay on the curve

$$\Gamma_k(s) = \{(u_k(s,x), v_k(s,x), w_k(s,x), \chi_k(s)) | s \in (-\epsilon, \epsilon)\}.$$

Proof. Let $z = (u,v,w)^T$, $\tilde{z} = (\tilde{u}, \tilde{v}, \tilde{w})^T$. Then (20) is equivalent to

$$D_z\mathcal{F}(\tilde{z}, \chi_3)(z) = \mathcal{A}_0 z'' + F_0(x, z, z'). \tag{22}$$

Here,

$$\mathcal{A}_0 = \begin{pmatrix} d_1 & 0 & 0 \\ 0 & d_2 & \chi_1\tilde{v} \\ -\chi_2\tilde{w} & -\chi_3\tilde{w} & d_3 \end{pmatrix},$$

and

$$F_0(x,z,z') = \begin{pmatrix} \tilde{f}_u u + \tilde{f}_v v + \tilde{f}_w w \\ \chi_1(\tilde{v}'w' + (\tilde{w}'v)') + \tilde{g}_u u + \tilde{g}_v v + \tilde{g}_w w \\ -\chi_2(\tilde{w}'u' + (\tilde{u}'w)') - \chi_3(\tilde{w}'v' + (\tilde{v}'w)') + \tilde{h}_u u + \tilde{h}_v v + \tilde{h}_w w \end{pmatrix}.$$

Since $d_i > 0$, $\chi_i > 0$; then (22) is strictly elliptic, and it satisfies Agmons's condition according to Remark 2.5 of Case 2 with $N = 1$ in [27]. Therefore, (22) is a Fredholm operator with zero index thanks to Theorem 3.3 and Remark 3.4 in [27]. The necessary condition for the existence of bifurcation is that the null space of $D_z\mathcal{F}(z^*,\chi)(z)$ is nonempty, where $z^* = (u^*, v^*, w^*)^T$. By taking $\tilde{z} = z^*$ in (20), one has

$$D_z\mathcal{F}(z^*,\chi_3)(z) = \begin{pmatrix} d_1u'' + f_u^*u + f_v^*v + f_w^*w \\ d_2v'' + \chi_1v^*w'' + g_u^*u + g_v^*v + g_w^*w \\ d_3w'' - \chi_2w^*u'' - \chi_3w^*v'' + h_u^*u + h_v^*v + h_w^*w \end{pmatrix}. \tag{23}$$

Its null space consists of solutions for the following system:

$$\begin{array}{ll} d_1u'' + f_u^*u + f_v^*v + f_w^*w = 0, & x \in \Omega, t > 0, \\ d_2v'' + \chi_1v^*w'' + g_u^*u + g_v^*v + g_w^*w, & x \in \Omega, t > 0, \\ d_3w'' - \chi_2w^*u'' - \chi_3w^*v'' + h_u^*u + h_v^*v + h_w^*w, & x \in \Omega, t > 0, \\ u' = v' = w' = 0, & x \in \partial\Omega, t > 0. \end{array} \tag{24}$$

Because Problem (24) is linear, we now consider the solution $z(x) = (u(x), v(x), w(x))$ of (24) in the form

$$z = \sum_{k=0}^{\infty} Z_k \cos kx, \quad k = n\pi,$$

where $Z_k = (U_k, V_k, W_k)$ are the Fourier coefficients. Substituting these series into (24) gives rise to

$$\begin{pmatrix} -d_1k^2 + f_u^* & f_v^* & f_w^* \\ g_u^* & -d_2k^2 + g_v^* & -\chi_1v^*k^2 + g_w^* \\ \chi_2w^*k^2 + h_u^* & \chi_3w^*k^2 + h_v^* & -d_3k^2 + h_w^* \end{pmatrix} \begin{pmatrix} U_k \\ V_k \\ W_k \end{pmatrix} = \begin{pmatrix} 0 \\ 0 \\ 0 \end{pmatrix}. \tag{25}$$

There exists a nontrivial solution $Z_k = (U_k, V_k, W_k)$ of (25) if the coefficient matrix in (25) is singular. For each $k > 0$, this condition holds if there exists positive $\chi_3 = \chi_k$, where

$$\chi_k = \frac{A_1k^6 + A_2k^4 + A_3k^2 + p_0}{w^*(B_1k^6 + B_2k^4 + B_3k^2)}, \tag{26}$$

with

$$\begin{array}{l} A_1 = d_1d_2d_3, \quad A_2 = -d_1d_2h_w^* - d_1d_3g_v^* - d_2d_3f_u^* + \chi_1v^*d_1h_v^* + \chi_1\chi_2v^*w^*f_v^* - d_2\chi_2w^*f_w^*, \\ A_3 = d_1(g_v^*h_w^* - g_w^*h_v^*) + d_2(f_u^*h_w^* - f_w^*h_u^*) + d_3(f_u^*g_v^* - f_v^*g_u^*) + \chi_1v^*(f_v^*h_u^* - f_u^*h_v^*) + \chi_2w^*(f_w^*g_v^* - f_v^*g_w^*), \\ B_1 = -d_1\chi_1v^*, \quad B_2 = d_1g_w^* + \chi_1v^*f_u^*, \quad B_3 = f_w^*g_u^* - f_u^*g_w^*. \end{array}$$

Moreover, we have that $\dim\mathcal{N}(D_z\mathcal{F}(z^*,\chi_k)) = 1$, where $\mathcal{N}$ denotes the null space, and $\mathcal{N}(D_z\mathcal{F}(z^*,\chi_k)) = span\{z_k\}$, where

$$z_k = (u_k, v_k, w_k)^T = \begin{pmatrix} 1 \\ V_k \\ W_k \end{pmatrix} \cos kx, \tag{27}$$

with

$$\bar{V}_k = \frac{d_1\chi_1 v^* k^4 - (\chi_1 v^* f_u^* + d_1 g_w^*)k^2 + f_u^* g_w^* - f_w^* g_u^*}{(\chi_1 v^* f_v^* - d_2 f_w^*)k^2 + f_w^* g_v^* - f_v^* g_w^*},$$
$$\bar{W}_k = -\frac{d_1 d_2 k^4 - (d_1 g_v^* + d_2 f_u^*)k^2 + f_u^* g_v^* - f_v^* g_u^*}{(\chi_1 v^* f_v^* - d_2 f_w^*)k^2 + f_w^* g_v^* - f_v^* g_w^*}.$$

Then, in accordance with bifurcation from the simple eigenvalue [26], to prove the theorem, it remains to show the validity of the following transversality condition

$$\frac{d}{d\chi_3} D_z \mathcal{F}(z^*, \chi)(z_k)|_{\chi_3=\chi_k} \notin Range(D_z \mathcal{F}(z^*, \chi_k)). \tag{28}$$

Differentiating (23) with respect to χ_3, we get

$$\frac{d}{d\chi_3} D_z \mathcal{F}(z^*, \chi)(z_k)|_{\chi_3=\chi_k} = \begin{pmatrix} 0 \\ 0 \\ -w^* v_k'' \end{pmatrix}.$$

Suppose that condition (28) fails. Then, there exists a nontrivial $\tilde{z} = (\tilde{u}, \tilde{v}, \tilde{w})^T$ such that

$$\begin{pmatrix} d_1\tilde{u}'' + f_u^*\tilde{u} + f_v^*\tilde{v} + f_w^*\tilde{w} \\ d_2\tilde{v}'' + \chi_1 v^*\tilde{w}'' + g_u^*\tilde{u} + g_v^*\tilde{v} + g_w^*\tilde{w} \\ d_3\tilde{w}'' - \chi_2 w^*\tilde{u}'' - \chi_3 w^*\tilde{v}'' + h_u^*\tilde{u} + h_v^*\tilde{v} + h_w^*\tilde{w} \end{pmatrix} = \begin{pmatrix} 0 \\ 0 \\ -w^* v_k'' \end{pmatrix}. \tag{29}$$

Let $\tilde{z} = \sum_{k=0}^{\infty} \tilde{Z}_k \cos kx$, where $\tilde{Z}_k = (\tilde{U}_k, \tilde{V}_k, \tilde{W}_k)$. Substituting these series into (29) gives rise to

$$\begin{pmatrix} -d_1k^2 + f_u^* & f_v^* & f_w^* \\ g_u^* & -d_2k^2 + g_v^* & -\chi_1 v^* k^2 + g_w^* \\ \chi_2 w^* k^2 + h_u^* & \chi_3 w^* k^2 + h_v^* & -d_3k^2 + h_w^* \end{pmatrix} \begin{pmatrix} \tilde{U}_k \\ \tilde{V}_k \\ \tilde{W}_k \end{pmatrix} = \begin{pmatrix} 0 \\ 0 \\ -w^* k^2 \end{pmatrix}. \tag{30}$$

We observe that the coefficient matrix in (30) with $\chi_3 = \chi_k$ is singular, while the right-hand side is nonzero: then this leads to a contradiction. Consequently, the transversality condition (28) is verified. Then, according to the Crandall–Rabinowitz bifurcation theory [26], there exist nonconstant positive solutions $(u_k(s,x), v_k(s,x), w_k(s,x), \chi_k(s))$ that can be parameterized as

$$\begin{aligned} &(u_k(s,x), v_k(s,x), w_k(s,x)) = (u^*, v^*, w^*) + s(1, \bar{V}_k, \bar{W}_k)\cos kx + s(\xi_k(s,x), \zeta_k(s,x), \eta_k(s,x)), \\ &\chi_k(s) = \chi_k + s\mathcal{K}_1 + s^2\mathcal{K}_2 + O(s^3), \end{aligned} \tag{31}$$

where $\mathcal{K}_i$ are constants, $(\xi_k(s,x), \zeta_k(s,x), \eta_k(s,x))$ is an element in the closed complement $\mathcal{Z}$ of $\mathcal{N}(D_{(u,v,w)}\mathcal{F}(u^*, v^*, w^*, \chi_k))$ in $\mathcal{X} \times \mathcal{X} \times \mathcal{X}$:

$$\mathcal{Z} = \left\{ z \in \mathcal{X} \times \mathcal{X} \times \mathcal{X} \Big| \int_0^1 z z_k dx = 0 \right\},$$

with $(\xi_k(0,x), \zeta_k(0,x), \eta_k(0,x)) = (0,0,0)$, and z_k given in (27).

Finally, we require $\chi_k \neq \chi_j$ for all positive $k \neq j$ in order to apply the bifurcation theory from a simple eigenvalue; therefore,

$$\frac{A_1k^6 + A_2k^4 + A_3k^2 + p_0}{w^*(B_1k^6 + B_2k^4 + B_3k^2)} \neq \frac{A_1j^6 + A_2j^4 + A_3j^2 + p_0}{w^*(B_1j^6 + B_2j^4 + B_3j^2)},$$

which is equivalent to (21). □

4. Pattern Formation

4.1. Conditions for Turing Instability

In this section, the effect of taxis on pattern formation is studied. According to Theorem 1, positive equilibrium E^* loses its stability through bifurcation as χ_3 crosses the critical bifurcation value χ_k. It is widely known that a reaction–diffusion system with two or more agents with largely different diffusion coefficients can generate spatially

heterogeneous patterns. The aim of this study is to investigate the occurrence of stationary patterns as a result of taxis pressure. Therefore, I consider a special case of Model (3) with equal diffusion coefficients for all components: $d_1 = d_2 = d_3 = d$, and resource-tactic sensitivity depends on prey-tactic coefficient $\chi_2 = \eta\chi_3 = \eta\chi$. Turing bifurcation occurs when $r_0(k^2) = 0$, which is analogous to

$$\chi_k = -\frac{1}{w^*}\frac{d^3k^6 + d(dp_2 + \chi_1 v^*h_v^*)k^4 + (dp_1 + \chi_1 v^*(f_v^*h_u^* - f_u^*h_v^*))k^2 + p_0}{d\chi_1 v^*k^6 + (\chi_1 v^*(\eta f_v^* - f_u^*) - d(\eta f_w^* + g_w^*))k^4 + (\eta(f_w^*g_v^* - f_v^*g_w^*) + f_u^*g_w^* - f_w^*g_u^*)k^2}. \quad (32)$$

Note that (32) is equivalent to (26). Then System (3) undergoes Turing instability when $r_0(k^2) < 0$ for some $k^2 > 0$. If the denominator in (32) is negative (positive), then $r_0(k^2) < 0$ is analogous to $\chi > \max\limits_k \chi_k$ ($\chi < \min\limits_k \chi_k$). The following theorem provides sufficient conditions for Turing instability.

Theorem 2. *System (3) undergoes Turing instability around the uniform steady-state* $E^* = (u^*, v^*, w^*)$ *if one of the following sets of conditions holds:*

1. $G_1(\eta - \eta_1) < 0$ *and* $\chi > \chi_{T1}$;
2. $G_1(\eta - \eta_1) > 0$, $\chi > \chi_{T2}$, *and there exist* $\chi_1 > \bar{\chi}_1$, $\eta > \eta_2$ *such that* $G_3 > 0$.

Here, G_1, G_3, η_1, η_2, *and* $\bar{\chi}_1, \chi_{T1}, \chi_{T2}$ *can be found in the proof of the theorem.*

Proof. Note that $r_0(k^2 = 0) = p_0 > 0$ and $\lim\limits_{k^2\to\infty} r_0(k^2) = \infty$. Then $r_0(k^2) < 0$ for some $k^2 > 0$ if $s_{02} < 0$ or $s_{01} < 0$. In this case the equation $r_0(k^2) = 0$ either possesses no positive roots or has two positive roots: namely, $0 < k_1^2 < k_2^2$ and $r_0(k^2) < 0$ for all $k^2 \in (k_1^2, k_2^2)$. The coefficients s_{01} and s_{02} can be rewritten as:

$$\begin{aligned} s_{01} &= \bar{S}_1 + \chi w^* G_1(\eta - \eta_1), \\ s_{02} &= \bar{S}_2 + \chi w^* v^* f_v^*(\eta - \eta_2)(\chi_1 - \bar{\chi}_1), \end{aligned}$$

where

$$\begin{aligned} \bar{S}_1 &= dp_1 + \chi_1 v^*(f_v^*g_u^* - f_u^*h_v^*), \\ \bar{S}_2 &= d(dp_2 + \chi_1 v^*h_v^*), \\ G_1 &= f_w^*g_v^* - f_v^*g_w^*, \quad \eta_1 = \tfrac{f_w^*g_u^* - f_u^*g_w^*}{G_1}, \\ \bar{\chi}_1 &= \tfrac{d(\eta f_w^* + g_w^*)}{v^* f_v^*(\eta - \eta_2)}, \quad \eta_2 = f_u^*/f_v^*. \end{aligned}$$

Let us introduce the following notation:

$$\begin{aligned} \chi_{T1} &= -\tfrac{\bar{S}_1}{w^* G_1(\eta - \eta_1)}, \\ \chi_{T2} &= -\tfrac{\bar{S}_2}{w^* v^* f_v^*(\eta - \eta_2)(\chi_1 - \bar{\chi}_1)}. \end{aligned}$$

Then $s_{01} < 0$ if $\chi > \chi_{T1}$ when $G_1(\eta - \eta_1) < 0$ or $\chi < \chi_{T1}$ when $G_1(\eta - \eta_1) > 0$; $s_{02} < 0$ if $\chi > \chi_{T2}$ when $(\eta - \eta_2)(\chi_1 - \bar{\chi}_1) > 0$ or $\chi < \chi_{T2}$ when $(\eta - \eta_2)(\chi_1 - \bar{\chi}_1) < 0$ since $f_v^* < 0$.

Consider the following limit:

$$R(k, \chi_1) = \lim_{\chi\to\infty} \tfrac{r_0(k^2)}{\chi w^*} = \quad d\chi_1 v^*k^6 + v^* f_v^*(\eta - \eta_2)(\chi_1 - \bar{\chi}_1)k^4 + G_1(\eta - \eta_1)k^2.$$

If $R(k, \chi_1) < 0$ for some $k^2 > 0$, then there exists $\tilde{\chi}_T$ such that System (3) undergoes Turing instability when $\chi > \tilde{\chi}_T$. Let $G_1(\eta - \eta_1) > 0$. If there exist $\chi_1 > \bar{\chi}_1$ and $\eta > \eta_2$ such that $G_3 > 0$, then $R(k, \chi_1) < 0$ for all $k_1^2 < k^2 < k_2^2$, where

$$k_1^2 = \frac{v^* f_v^*(\eta - \eta_2)(\chi_1 - \bar{\chi}_1) - \sqrt{G_3}}{2d\chi_1 v^*}, \quad k_2^2 = \frac{v^* f_v^*(\eta - \eta_2)(\chi_1 - \bar{\chi}_1) + \sqrt{G_3}}{2d\chi_1 v^*},$$

and

$$G_3 = (v^* f_v^* (\eta - \eta_2)(\chi_1 - \bar{\chi}_1))^2 - 4\chi_1 v^* d G_1 (\eta - \eta_1).$$

If $\eta < \eta_2$, then $\bar{\chi}_1 < 0$, so $\chi_1 < \bar{\chi}_1$ is not valid. Let $G_1(\eta - \eta_1) < 0$, then $R(k, \chi_1) < 0$ for all $0 < k^2 < k_2^2$ and $\chi_1 > 0$. □

4.2. Conditions for Wave Instability

In three-component models, not only can Turing bifurcation occur, but wave bifurcation (or finite wavenumber Hopf bifurcation) can also occur. Wave bifurcation breaks spatial and temporal symmetries, and the system generates patterns that are oscillatory in space and time. This bifurcation occurs when $r(k^2) = r_1(k^2) r_2(k^2) - r_0(k^2) = 0$, which is analogous to

$$r(k^2) = q_3 (k^2)^3 + q_2 (k^2)^2 + q_1 k^2 + p_1 p_2 - p_0 = 0, \tag{33}$$

where $q_3 = 8d^3 + 2d\chi_1\chi_3 v * w*$, $q_2 = 8d^2 p_2 - \chi_3 w^* (2d(\eta f_w^* + g_w^*) + \chi_1 v^* (\eta f_v^* + g_v^* + h_w^*)) + 2d\chi_1 v^* h_v^*$, $q_1 = 2d(p_2^2 + p_1) + \chi_3 w^* (\eta (f_u^* f_w^* + f_v^* g_w^* + f_w^* h_w^*) + f_w^* g_u^* + g_v^* g_w^* + g_w^* h_w^*) - \chi_1 v^* (f_v^* g_u^* + g_v^* h_v^* + h_v^* h_w^*)$. Condition (33) is equivalent to

$$\chi = \chi_k^W = -\frac{1}{w^*} \frac{8d^3 k^6 + \bar{Q}_2 k^4 + \bar{Q}_1 k^2 + p_1 p_2 - p_0}{2d\chi_1 v^* k^6 - v^* f_v^* (\eta - \eta_4)(\chi_1 - \tilde{\chi}_1) k^4 + G_4 (\eta - \eta_3) k^2}, \tag{34}$$

where

$$\begin{aligned}
&\bar{Q}_1 = 2d(p_2^2 + p_1) - \chi_1 v^* (f_v^* g_u^* + g_v^* h_v^* + h_v^* h_w^*), \quad \bar{Q}_2 = 2d(4d p_2 + \chi_1 v^* h_v^*), \\
&G_4 = f_u^* f_w^* + f_v^* g_w^* + f_w^* h_w^*, \quad \eta_3 = -\tfrac{f_w^* g_u^* + g_v^* g_w^* + g_w^* h_w^*}{G_4}, \\
&\eta_4 = -\tfrac{g_v^* + h_w^*}{f_v^*}, \quad \tilde{\chi}_1 = -\tfrac{2d(\eta f_w^* + g_w^*)}{v^* f_v^* (\eta - \eta_4)}.
\end{aligned}$$

Then System (3) undergoes wave instability when $r(k^2) < 0$ for some $k^2 > 0$. If the denominator in (34) is negative (positive), then $r(k^2) < 0$ is analogous to $\chi > \max\limits_k \chi_k^W$ ($\chi < \min\limits_k \chi_k^W$). The following theorem provides sufficient conditions for wave instability.

Theorem 3. *System (3) undergoes wave instability around the uniform steady-state $E^* = (u^*, v^*, w^*)$ if one of the following sets of conditions holds:*

1. $G_4(\eta - \eta_3) < 0$ *and* $\chi > \chi_{W1}$;
2. $G_4(\eta - \eta_3) > 0$, $\chi > \chi_{W2}$, *and there exist* $\chi_1 > \tilde{\chi}_1$ *and* $\eta < \eta_4$ *such that* $G_5 > 0$.

Here, G_4, G_5, η_3, η_4, and χ_{W1}, χ_{W2} can be found in the proof of the theorem.

Proof. The proof is similar to that of Theorem 2. Since $r(k^2 = 0) = p_1 p_2 - p_0 > 0$ and $\lim\limits_{k^2 \to \infty} r(k^2) = \infty$, then $r_0(k^2) < 0$ for some $k^2 > 0$ if $q_2 < 0$ or $q_1 < 0$. The coefficients q_1 and q_2 can be written as:

$$\begin{aligned}
q_1 &= \bar{Q}_1 + \chi w^* G_4 (\eta - \eta_3), \\
q_2 &= \bar{Q}_2 - \chi w^* v^* f_v^* (\eta - \eta_4)(\chi_1 - \tilde{\chi}_1).
\end{aligned}$$

Let us introduce the following notation:

$$\begin{aligned}
\chi_{W1} &= -\tfrac{\bar{Q}_1}{w^* G_4 (\eta - \eta_3)}, \\
\chi_{W2} &= \tfrac{\bar{Q}_2}{w^* v^* f_v^* (\eta - \eta_4)(\chi_1 - \tilde{\chi}_1)}.
\end{aligned}$$

Then $q_1 < 0$ if $\chi > \chi_{W1}$ when $G_4(\eta - \eta_3) < 0$ or $\chi < \chi_{W1}$ when $G_4(\eta - \eta_3) > 0$; $q_2 < 0$ if $\chi > \chi_{W2}$ when $(\eta - \eta_4)(\chi_1 - \tilde{\chi}_1) < 0$ or $\chi < \chi_{W2}$ when $(\eta - \eta_4)(\chi_1 - \tilde{\chi}_1) > 0$ since $f_v^* < 0$.

Consider the following limit:

$$R_1(k,\chi_1) = \lim_{\chi\to\infty} \frac{r(k^2)}{\chi w^*} = \quad 2d\chi_1 v^* k^6 - v^* f_v^*(\eta-\eta_4)(\chi_1-\tilde{\chi}_1)k^4 + G_4(\eta-\eta_3)k^2.$$

If $R_1(k,\chi_1) < 0$ for some $k^2 > 0$, then there exists $\tilde{\chi}_W$ such that System (3) undergoes wave instability when $\chi > \tilde{\chi}_W$. Let $G_4(\eta-\eta_3) > 0$. If there exist $\chi_1 > \tilde{\chi}_1$ and $\eta < \eta_4$ such that $G_5 > 0$, then $R_1(k,\chi_1) < 0$ for all $k_1^2 < k^2 < k_2^2$, where

$$k_1^2 = \frac{v^* f_v^*(\eta-\eta_4)(\chi_1-\tilde{\chi}_1) - \sqrt{G_5}}{4d\chi_1 v^*}, \quad k_2^2 = \frac{v^* f_v^*(\eta-\eta_4)(\chi_1-\tilde{\chi}_1) + \sqrt{G_5}}{4d\chi_1 v^*},$$

and

$$G_5 = (v^* f_v^*(\eta-\eta_4)(\chi_1-\tilde{\chi}_1)^2 - 4\chi_1 v^* d G_4(\eta-\eta_3).$$

If $\eta > \eta_4$, then $\tilde{\chi}_1 < 0$, so $\chi_1 < \tilde{\chi}_1$ is not valid. Let $G_1(\eta-\eta_1) < 0$; then $R(k,\chi_1) < 0$ for all $0 < k^2 < k_2^2$ and $\chi_1 > 0$. □

5. Numerical Simulations

5.1. Numerical Scheme

I simulated System (4) using the method of lines with an $n = 100$-point spatial grid for a domain $[0,1]$, i.e., $(u_i, v_i, w_i)(t) = (u, v, w)(i\Delta x, t)$, $i = 0, \ldots, n$, and $\Delta x = h = 0.01$. For spatial discretization, the second-order central difference is used for the diffusive terms:

$$\begin{aligned}
\tfrac{dz_i}{dt} &= \tfrac{d}{h^2}(z_{i+1} - 2z_i + z_{i-1}) + F_i, \quad i = 1, \ldots, n-1,\\
\tfrac{dz_0}{dt} &= \tfrac{2d}{h^2}(z_1 - z_0) + F_0,\\
\tfrac{dz_n}{dt} &= -\tfrac{2d}{h^2}(z_n - z_{n-1}) + F_n,
\end{aligned}$$

where $z_i(t) = (u_i(t), v_i(t), w_i(t))$, $F_i = (f(z_i), g(z_i), h(z_i))$, and the first-order upwind scheme is used for the taxis terms:

$$\begin{aligned}
\tfrac{dz_i}{dt} &= \tfrac{1}{h}(Q_{i+1/2} - Q_{i-1/2}), \quad i = 1, \ldots, n-1,\\
\tfrac{dz_0}{dt} &= -\tfrac{2}{h} Q_{1/2},\\
\tfrac{dz_n}{dt} &= \tfrac{2}{h} Q_{n-1/2},
\end{aligned}$$

where $Q_{i+1/2} = z_i s_{i+1}$ if $s_{i+1} > 0$ and $Q_{i+1/2} = z_{i+1} s_{i+1}$ if $s_{i+1} \le 0$; $s_i = (0, \frac{S_i' - S_{i-1}'}{h}, \frac{S_i'' - S_{i-1}''}{h})$, $S_i' = \chi_1 w_i(t)$, $S_i'' = -(\chi_2 u_i(t) + \chi_3 v_i(t))$. The result of spatial discretization is the autonomous semi-discrete system:

$$z'(t) = G(z(t)), \quad z(0) = z_0, \quad t \in [0, T]. \tag{35}$$

The splitting method [28,29] is used for solving this system. The function $G(z)$ is split as $G(z) = G_1(z) + G_2(z)$, where function G_1 contains the taxis term, and G_2 contains the diffusion and reaction terms. In the time integration, the taxis term is treated explicitly, and the remaining terms are treated linearly implicitly by approximate matrix factorization and operator splitting. Then, given an approximation $y = z^n$ at time t_n and a step size τ, we compute

$$\hat{y} = \Gamma_1(\frac{\tau}{2}, t_n + \frac{\tau}{2})\Gamma_2(\tau, t_n)\Gamma_1(\frac{\tau}{2}, t_n)y. \tag{36}$$

Here Γ_1 and Γ_2 are approximate evolution operators of G_1 and G_2, respectively. Specifically, $\Gamma_1(\tau/2, t_n)y$ approximates the solution of the initial-value problem $z' = G_1(z(t))$, $t \ge t_n$, $z(t_n) = y$. As a result, we obtain $\hat{y}^{(1)}$. For approximation of Γ_1, the Runge–Kutta fourth-order method is used. Then, $\Gamma_2(\tau, t_n)\hat{y}^{(1)}$ approximates the solution of the initial-value problem $z' = G_2(z(t))$, $t \ge t_n$, $z(t_n) = \hat{y}^{(1)}$. The right-hand side of the ODE can be written as $G_2 = G_{2a} + G_{2b}$, where G_{2a} contains the terms arising from the discretization

of diffusion terms, and G_{2b} contains the reaction terms. A linearly implicit variant of the trapezoidal splitting method was used for approximation of Γ_2:

$$\begin{aligned}
\tilde{y}^{(1)} &= \hat{y}^{(1)} + \tfrac{\tau}{2} G_{2a}(\hat{y}^{(1)}),\\
\tilde{y}^{(2)} &= \tilde{y}^{(1)} + \tfrac{\tau}{2} G_{2b}(\tilde{y}^{(1)}),\\
\tilde{y}^{(3)} &= \tilde{y}^{(2)} + \tfrac{\tau}{2}(I - \tfrac{\tau}{2} T_{2b})^{-1} G_{2b}(\tilde{y}^{(2)}),\\
\hat{y}^{(2)} &= \tilde{y}^{(3)} + \tfrac{\tau}{2}(I - \tfrac{\tau}{2} T_{2a})^{-1} G_{2a}(\tilde{y}^{(3)}).
\end{aligned}$$

Here, $T_{2a} = J_{2a}(\tilde{y}^{(3)}) + \mathcal{O}(\tau)$, $T_{2b} = J_{2b}(\tilde{y}^{(2)}) + \mathcal{O}(\tau)$ are first-order approximations of the Jacobians J_{2a} and J_{2b} of G_{2a} and G_{2b}, respectively. The solution to Problem (36) is obtained by again using the operator Γ_1: $\hat{y} = \Gamma_1(\frac{\tau}{2}, t_n + \frac{\tau}{2})\hat{y}^{(2)}$. The approximation (36) is consistent with order two (see [28]).

5.2. Spatiotemporal Patterns

Now, I investigate the effect of prey- and predator-taxis on the formation of stationary and oscillatory patterns. In the simulations to be presented below, I have taken the following parameters: $\gamma_1 = 0.3, \gamma_2 = 0.4, \gamma_3 = 0.5$, $m_1 = m_2 = 0.1$, $\mu_1 = 0.3, \mu_2 = 0.1$, $\mu_3 = 0.3$, $\mu_4 = 0.15$, $\delta_1 = 0.1, \delta_2 = 0.2$, $d = 10^{-4}$. For the given set of parameter values, the equilibrium point $E^* = (0.31, 0.38, 0.05)$ for the spatially homogeneous model is stable. The initial condition is always the steady-state with small perturbations: $u(x,0) = u^* + \xi_1, v(x,0) = v^* + \xi_2$, $w(x,0) = w^* + \xi_3$, where ξ_i are small-amplitude random perturbations at one percent from the steady-state E^*.

In accordance with Theorem 2, we get the following conditions for Turing instability:

$$\eta > 0.68, \quad \chi_1 > 0, \quad \chi > \frac{2 \cdot 10^{-5} - 7.5\chi_1}{\eta - 0.68},$$

or

$$0 < \eta < 0.68, \quad \chi_1 > \frac{6.6 \cdot 10^{-7} + 2.2 \cdot 10^{-6}\eta}{\eta + 0.06}, \quad \chi > \frac{10^{-12} + 1.9 \cdot 10^{-7}\chi_1}{-6.6 \cdot 10^{-7} + \eta(-2.2 \cdot 10^{-6} + \chi_1) + 0.06\chi_1}.$$

In accordance with Theorem 3, we get the conditions for wave instability as

$$0 < \eta < 0.61, \quad \chi_1 > 0, \quad \chi > \frac{-4 \cdot 10^{-5} - 6.9\chi_1}{\eta - 0.61}.$$

Figure 1 shows stability/instability domains with $\chi_1 = 0, 0.01, 0.1, 1$. When $\chi_1 = 0$, the system undergoes wave instability (domain Ω_3) for small η. Turing bifurcation occurs if $\eta > 0.68$ (domain Ω_2). When $\chi_1 \neq 0$, the system undergoes Turing instability for almost all $(\eta, \chi) > 0$. The right panel in Figure 1 shows the wave bifurcation curves for $\chi_1 = 0.01, 0.1, 1$; instability occurs below these curves. Both instabilities are possible when $(\eta, \chi) \in \Omega_4$.

Figure 2 demonstrates the system dynamics for $\eta = 0$ and $\chi = 2$ and three variants of χ_1. When $\chi_1 = 0$, the system undergoes wave instability. The top panel in the figure shows that after a long period of spatially homogeneous oscillations, a standing wave regime is established. With an increase in χ, both instabilities are possible. The system generates standing waves (middle panel) and a stationary structure (bottom panel) when $\chi_1 = 0.1$ and $\chi_1 = 2$, respectively.

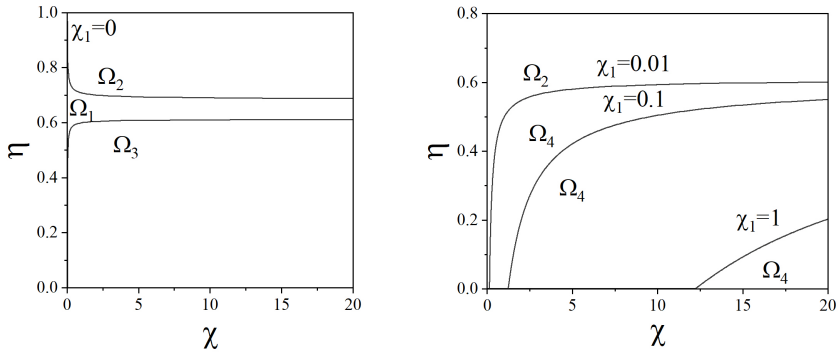

Figure 1. Stability/instability domains: Ω_1—stability area, Ω_2—Turing instability, Ω_3—wave instability, and Ω_4—Turing and wave instabilities.

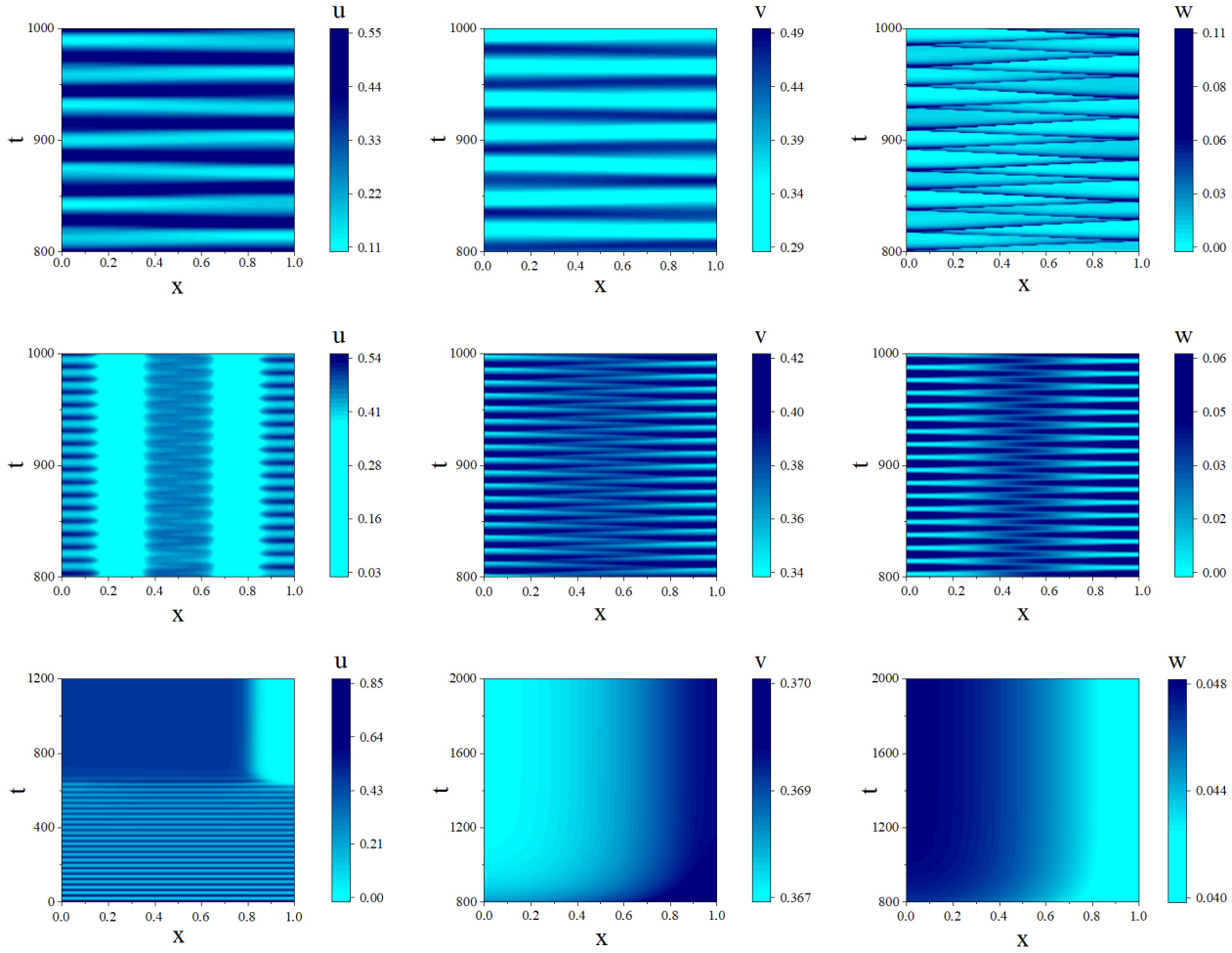

Figure 2. Stationary and oscillatory patterns for $\eta = 0$ and $\chi = 2$. Top panel: $\chi_1 = 0$; middle panel: $\chi_1 = 0.1$; bottom panel: $\chi_1 = 2$.

Figure 3 shows the spatial patterns for $\eta \neq 0$; in this case, Turing and wave bifurcations are possible. For $\eta = 0.05$ and $\eta = 0.5$, after a certain incubation period, stationary patterns emerge. When $\eta > 0.61$, only Turing bifurcation occurs. Figure 4 demonstrates the system dynamics for $\eta = 1$ and $\eta = 2$. For $\eta = 1$ ($\chi_2 = 2$), the system generates a spatiotemporal pattern oscillating in space and time (top panel). This behavior indicates that nonlinear effects arising from the interaction between the Turing and wave modes cause the pure

Turing mode to lose its stability before the wave bifurcation occurs. With an increase in η, the spatial structures achieve equilibrium (bottom panel).

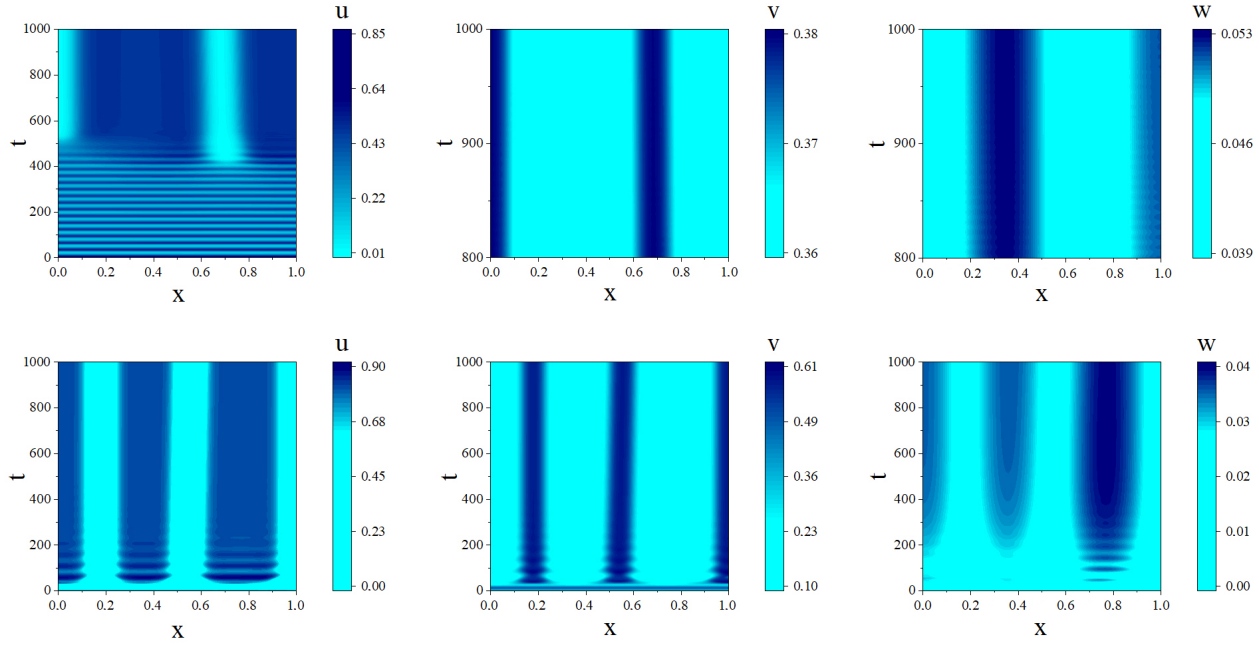

Figure 3. Stationary and oscillatory patterns for $\chi = 2$, $\chi_1 = 0.1$. Top panel: $\chi_2 = 0.1$; bottom panel: $\chi_2 = 1$.

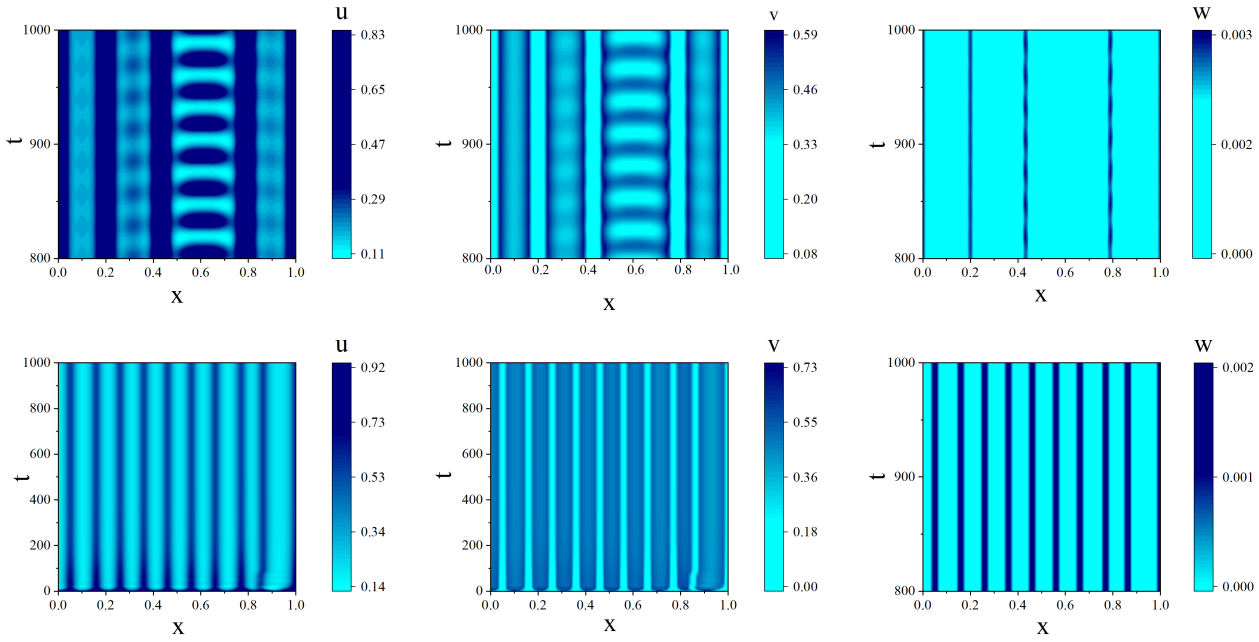

Figure 4. System dynamics for $\chi = 2$, $\chi_1 = 0.1$. Top panel: $\chi_2 = 2$; bottom panel: $\chi_2 = 4$.

The initial condition for all the simulations discussed above is the stable spatially homogeneous equilibrium with small perturbations. Now, consider the system dynamics when taking an unstable spatially homogeneous equilibrium as the initial state. In the simulations to be presented below, I have taken the same set of parameter values as in the previous ones; the only exceptions are $\mu_1 = 0.5$ and $\mu_2 = 0.2$. For the given set of parameter values, the equilibrium point $E^* = (0.13, 0.34, 0.04)$ for the spatially homogeneous model is unstable. Oscillatory dynamics of the system without diffusion

and taxis are presented in Figure 5a. As diffusion and taxis are incorporated into the system, the system behavior changes as follows. When only prey-taxis is considered, we observe a solution that is oscillatory in time and homogeneous in space (Figure 5b). When predator-taxis is considered, stationary structures are formed. Figure 6 demonstrates the solution to System (3) for $\chi_3 = 0.1$ and three variants of prey-taxis coefficients.

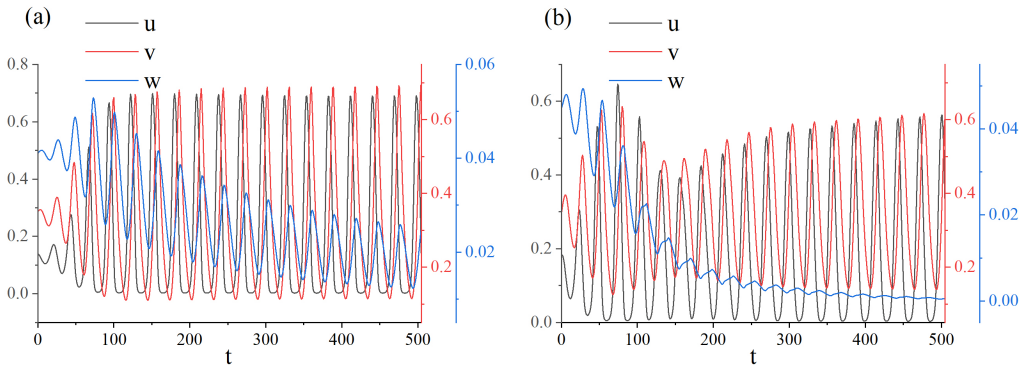

Figure 5. Spatially homogeneous solutions to System (3) with an unstable spatially homogeneous equilibrium as the initial state: (**a**) $d_i = 0$, $\chi = \chi_1 = \chi_2 = 0$; (**b**) $d_i = 10^{-4}$, $\chi = 0.5$, $\chi_1 = \chi_2 = 0$.

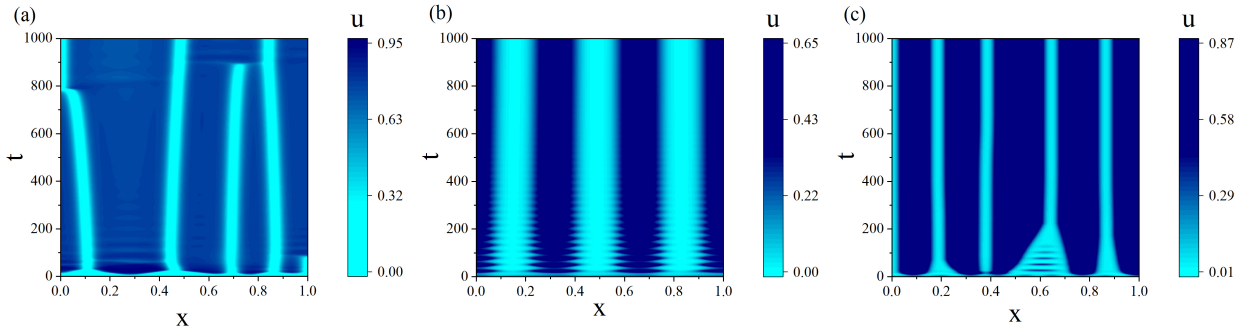

Figure 6. Spatially nonhomogeneous solutions to System (3) with an unstable spatially homogeneous equilibrium as the initial state with $\chi_1 = 0.1$: (**a**) $\chi = \chi_2 = 0$; (**b**) $\chi = 0.5$, $\chi_2 = 0.05$; (**c**) $\chi = 0.5$, $\chi_2 = 0.5$.

6. Discussion and Conclusions

This paper presents a model of a three-trophic food chain with an omnivorous predator and with consideration of spatial heterogeneity. The model considers the movements of the predator to be directed towards the areas with high densities of the resource and the prey, and the prey moves opposite to the gradient of the predator distribution. The proposed model provides a way to represent the dynamics of a community in which the predator can use different foraging strategies. This model, which takes into account the movement of the predator towards the gradient direction of both species' distributions, displays qualitatively different behavior of the system as the taxis coefficients change. Moreover, the model allows the assessment of the cumulative effect of prey-taxis and anti-predator mechanisms on the community dynamics.

A linear analysis of the system stability under small spatially inhomogeneous disturbances is carried out. The existence of a nonconstant positive equilibrium as a result of Turing bifurcation is proved. Sufficient conditions for Turing and wave instabilities are obtained. It is shown that the system can lose stability with a high level of prey-taxis. Analysis of the taxis coefficients' effects on the system dynamics reveals the following properties of the system.

If only the prey-taxis is considered, then either Turing or wave instability may occur depending on the resource-tactic rate. When the predator-taxis is taken into account, sta-

tionary structures are formed when the resource-tactic coefficient is high. If this parameter is less than the prey-tactic coefficient, then Turing patterns and wave modes may exist.

Numerical simulations reveal that an increase in χ_1 leads to a regime shift in which oscillations in the population abundances change to equilibrium spatially heterogeneous structures. A further increase in χ_1 at a fixed η does not lead to a change in the stationary structures. As η increases, the dynamics of the system achieve equilibrium, but the structures change along with changes to the resource-tactic coefficient. The real parts of the eigenvalues plotted in Figure 7 show that with increasing η, the range of wavenumbers for unstable modes and growth rates of these modes also increase. An increase in χ_1 leads only to growth of $Re(\lambda_k)$ for the most unstable mode, and the range of unstable wavenumbers practically does not change. From a biological point of view, as η increases, the predator switches its preference to the resource, and the fear-driven behavioral avoidance of predators forces prey competing for the resource and predator-free-area species to converge on a narrower suite of resource that is associated with low predation risk [30]. An increase in the predator-taxis sensitivity leads to an increase in the growth rates of the most unstable modes, resulting in a decrease in the incubation time for the structures to emerge, while the spatial distribution pattern remains virtually unchanged.

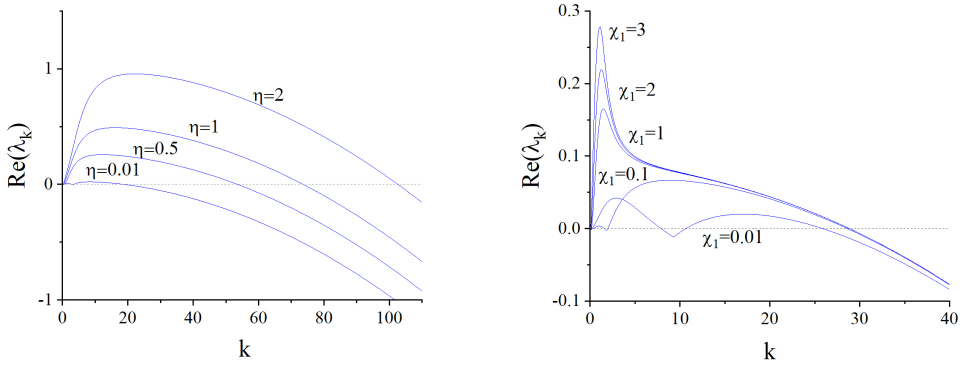

Figure 7. The real parts of the eigenvalues for Equation (15) as a function of k.

In real communities, such spatial heterogeneity can be caused by various reasons, both physical and biological. The heterogeneity of planktonic communities is initiated by turbulent advection [31] or the behavior of zooplankton in response to the presence of toxic phytoplankton [32]. The propagation of spatial waves caused by taxis is observed in bacterial populations responding to changes in the gradient of an attractant or repellent [33]. Wave solutions are demonstrated by models of the invasion of species [34] or infections [35].

The numerical simulations demonstrate a variety of system dynamics, including the formation of stable and unstable stationary and oscillatory patterns. When the parameters are selected from the Turing instability area and are close to the wave instability line, the purely stationary Turing structures become modulated (Figure 4). Similar system behavior was established in [36]. The stability of Turing structures depends on whether subcritical or supercritical bifurcation occurs; the determination of the nature of bifurcation requires a weakly nonlinear analysis. This analysis can also determine the type of wave—namely, a traveling or standing wave—that arises when a homogeneous steady state goes through that bifurcation (see [37] and references therein). Such nonlinear analysis is beyond the scope of this work, which has focused exclusively on studying the existence of a nonconstant steady state to the system and the patterns appearing at the onset of Turing and wave instability, but it will form the subject of future work by the present author.

As a final comment, I would like to note one more property of the presented model. A system's ability to form patterns is considered one of the mechanisms that allows species to coexist. The anti-predator behavior of prey promotes the formation of stationary structures. The effects of refuges used by prey increase the equilibrium density of the prey population. However, the presented model demonstrates a decline in the prey population with an

increase in predator-tactic sensitivity when resource-tactic sensitivity is low. This decline may be caused by the fact that prey aggregated in refuge habitats may strongly compete for limited resources [30]. With an increase in the resource-tactic coefficient, the prey population begins to grow, and the predator, whose diet consists mainly of the resource, begins to decline catastrophically. Nevertheless, the system stabilizes, and all species in the community survive.

Funding: This work was carried out within the framework of the state targets of the Institute of Automation and Control Processes of the Far Eastern Branch of the Russian Academy of Sciences.

Data Availability Statement: No new data were created or analyzed in this study. Data sharing is not applicable to this article.

Conflicts of Interest: The author declare no conflicts of interest.

References

1. Nathan, R.; Getz, W.M.; Revilla, E.; Holyoak, M.; Kadmon, R.; Saltz, D.; Smouse, P.E. A movement ecology paradigm for unifying organismal movement research. *Proc. Natl. Acad. Sci. USA* **2008**, *105*, 19052–19059. [CrossRef] [PubMed]
2. Quévreux, P.; Pigeault, R.; Loreau, M. Predator avoidance and foraging for food shape synchrony and response to perturbations in trophic metacommunities. *J. Theor. Biol.* **2021**, *528*, 110836. [CrossRef] [PubMed]
3. Holmes, E.E.; Lewis, M.A.; Banks, J.E.; Veit, R.R. Partial Differential Equations in Ecology: Spatial Interactions and Population Dynamics. *Ecology* **1994**, *75*, 17–29. [CrossRef]
4. Skellam, J.G. Random Dispersal in Theoretical Populations. *Biometrika* **1951**, *38*, 196–218. [CrossRef] [PubMed]
5. Kareiva, P.; Odell, G. Swarms of predators exhibit "preytaxis" if individual predators use area restricted search. *Am. Nat.* **1987**, *130*, 233–270. [CrossRef]
6. Berezovskaya, F.S.; Karev, G.P. Bifurcations of travelling waves in population taxis models. *Phys. Uspekhi* **1999**, *42*, 917–929. [CrossRef]
7. Turchin, P. *Quantitative Analysis of Movement: Measuring and Modeling Population Redistribution in Animals and Plants*; Sinauer Associates: Sunderland, MA, USA, 1998.
8. Wang, Q.; Song, Y.; Shao, L. Nonconstant positive steady states and pattern formation of 1d prey-taxis systems. *J. Nonlinear Sci.* **2017**, *27*, 71–97. [CrossRef]
9. Wang, X.; Wang, W.; Zhang, G. Global bifurcation of solutions for a predator–prey model with prey-taxis. *Math. Methods Appl. Sci.* **2015**, *38*, 431–443. [CrossRef]
10. Lee, J.M.; Hillen, T.; Lewis, M.A. Pattern formation in prey-taxis systems. *J. Biol. Dyn.* **2009**, *3*, 551–573. [CrossRef]
11. Tyutyunov, Y.V.; Titova, L.I.; Senina, I.N. Prey-taxis destabilizes homogeneous stationary state in spatial Gause–Kolmogorov-type model for predator–prey system. *Ecol. Complex.* **2017**, *31*, 170–180. [CrossRef]
12. Pang, P.Y.H.; Wang, M. Strategy and stationary pattern in a three-species predator–prey model. *J. Differ. Equ.* **2004**, *200*, 245–273. [CrossRef]
13. Wang, K.; Wang, Q.; Yu, F. Stationary and time-periodic patterns of two-predator and one-prey systems with prey-taxis. *Discret. Contin. Dyn. Syst.* **2017**, *37*, 505–543. [CrossRef]
14. Hamilton, W.D. Geometry of the selfish herd. *J. Theor. Biol.* **1971**, *31*, 295–311. [CrossRef]
15. Xiao, D.; Ruan, S. Codimension two bifurcations in a predator–prey system with group defense. *Int. J. Bifurc. Chaos* **2001**, *11*, 2123–2131. [CrossRef]
16. Hsu, S.B.; Ruan, S.; Yang, T.H. Analysis of three species Lotka–Volterra food web models with omnivory. *J. Math. Anal. Appl.* **2015**, *426*, 659–687. [CrossRef]
17. Kumari, S.; Upadhyay, R.K. Dynamics comparison between non-spatial and spatial systems of the plankton–fish interaction model. *Nonlinear Dyn.* **2020**, *99*, 2479–2503. [CrossRef]
18. Mortoja, S.G.; Panja, P.; Mondal, S.K. Stability Analysis of Plankton–Fish Dynamics with Cannibalism Effect and Proportionate Harvesting on Fish. *Mathematics* **2023**, *11*, 3011. [CrossRef]
19. Giricheva, E. Stability and bifurcation analysis of a tri-trophic food chain model with intraguild predation. *Int. J. Biomath.* **2023**, *16*, 2250073. [CrossRef]
20. Wu, C.J.; Chiang, K.P.; Liu, H. Diel feeding pattern and prey selection of mesozooplankton on microplankton community. *J. Exp. Mar. Biol. Ecol.* **2010**, *390*, 134–142. [CrossRef]
21. Fuest, M. Global Solutions near Homogeneous Steady States in a Multidimensional Population Model with Both Predator- and Prey-Taxis. *SIAM J. Math. Anal.* **2020**, *52*, 5865–5891. [CrossRef]
22. Wang, J.F.; Wu, S.N.; Shi, J.P. Pattern formation in diffusive predator-prey systems with predator-taxis and prey-taxis. *Discret. Contin. Dyn. Syst. Ser. B* **2021**, *26*, 1273–1289 [CrossRef]
23. Guo, X.; Wang, J. Dynamics and pattern formations in diffusive predator-prey models with two prey-taxis. *Math. Methods Appl. Sci.* **2019**, *42*, 4197–4212. [CrossRef]

24. Han, R.; Röst, G. Stationary and oscillatory patterns of a food chain model with diffusion and predator-taxis. *Math. Methods Appl. Sci.* **2023**, *46*, 9652–9675. [CrossRef]
25. Malchow, H.; Petrovskii, S.V.; Venturino, E. *Spatiotemporal Patterns in Ecology and Epidemiology: Theory, Models, and Simulation*; CRC Press: Boca Raton, FL, USA, 2007.
26. Crandall, M.G.; Rabinowitz, P.H. Bifurcation from simple eigenvalues. *J. Funct. Anal.* **1971**, *8*, 321–340. [CrossRef]
27. Shi, J.; Wang, X. On global bifurcation for quasilinear elliptic systems on bounded domains. *J. Differ. Equ.* **2009**, *246*, 2788–2812. [CrossRef]
28. Gerisch, A.; Griffiths, D.F.; Weiner, R.; Chaplain, M.A. A positive splitting method for mixed hyperbolic-parabolic systems. *Numer. Methods Partial. Differ. Equ. Int. J.* **2001**, *17*, 152–168. [CrossRef]
29. Hundsdorfer, W.H.; Verwer, J.G.; Hundsdorfer, W.H. *Numerical Solution of Time-Dependent Advection-Diffusion-Reaction Equations*; Springer: Berlin/Heidelberg, Germany, 2003; Volume 33.
30. Orrock, J.L.; Preisser, E.L.; Grabowski, J.H.; Trussell, G.C. The cost of safety: Refuges increase the impact of predation risk in aquatic systems. *Ecology* **2013**, *94*, 573–579. [CrossRef]
31. Abraham, E.R. The generation of plankton patchiness by turbulent stirring. *Nature* **1998**, *391*, 577–580. [CrossRef]
32. Semplice, M.; Venturino, E. Travelling waves in plankton dynamics. *Math. Model. Nat. Phenom.* **2013**, *8*, 64–79. [CrossRef]
33. Ivanitsky, G.R.; Medvinskii, A.B.; Tsyganov, M.A. From the dynamics of population autowaves generated by living cells to neuroinformatics. *Phys. Uspekhi* **1994**, *37*, 961–989. [CrossRef]
34. Morozov, A.; Petrovskii, S.; Li, B.L. Spatiotemporal complexity of patchy invasion in a predator-prey system with the Allee effect. *J. Theor. Biol.* **2006**, *238*, 18–35. [CrossRef] [PubMed]
35. Bate, A.M.; Hilker, F.M. Preytaxis and travelling waves in an eco-epidemiological model. *Bull. Math. Biol.* **2019**, *81*, 995–1030. [CrossRef] [PubMed]
36. Yang, L.A. Pattern formation arising from interactions between Turing and wave instabilities. *J. Chem. Phys.* **2002**, *117*, 7259–7265. [CrossRef]
37. Kaminaga, A.; Vanag, V.K.; Epstein, I.R. A reaction–diffusion memory device. *Angew. Chem.* **2006**, *45*, 3087–3089. [CrossRef]